XLIII CILAMCE
21–25, November, 2022
FOZ DO IGUAÇU – PR – BRAZIL

Yield design approach to uplift bearing capacity of shallow rectangular plate anchors

Mateus Forcelini[1], Samir Maghous[1]

[1]*Dept. of Civil Engineering, Federal University of Rio Grande do Sul*
Av. Osvaldo Aranha 99, 3rd floor, CEP 90035-190, Porto Alegre, RS, Brazil
forcelini.mateus@gmail.com, samir.maghous@ufrgs.com

Abstract. Plate anchors are a widely used class of foundation systems for structures subject to uplift forces. Its bearing capacity evaluation has been object of constant revisions in literature, notably as a result of the recent decommission operations of large offshore structures. In this context, the present paper aims to evaluate the uplift resistance of shallow rectangular plate anchors based on the theoretical framework of limit analysis and its related kinematic approach. Upper bound estimates of the collapse load are obtained from a class of failure mechanisms considering generic discontinuity surfaces defined from the functional minimization of the uplift bearing capacity. The rock is modeled as a Tresca material with a tension cut-off criterion, whereas the lower interface of the anchor exhibits a tensile stress threshold. A parametric study is conducted to evaluate the effect of the problem main parameters, allowing for an estimate of the ultimate pullout force for several cases. Finally, the semi-analytical predictions obtained are compared with available results in the literature, thus validating its application. Results show that model predictions are in good agreement with available results for plates with low embedment ratios. The dependence on the tensile stress limit of the Tresca material and the interface resistance are also highlighted.

Keywords: Plate anchors, Uplift bearing capacity, Limit analysis

1 Introduction

Plate anchors are widely adopted as foundation systems for structures subject to uplift forces, such as mooring systems for offshore oil and gas facilities, transmission towers, mining structures, dry docks, and storage tanks subject to flooding. More specifically, the subsea infrastructure adopted in the gas industry demands several instruments to be installed over the seabed (e.g. manifolds, terminations, sleepers, protection systems, etc.), which are usually supported by shallow foundations also named *mudmats*. These foundations are typically rectangular anchors with dimensions ranging from 2 to 40 m and embedment depth of about 5 to 50% of its width (Randolph et al. [1]).

Many of these offshore infrastructure has been in service for several decades and at some point reached or will reach its 'life-extension', raising concerns about its decommission operations demanded by several environmental protection agencies. Such extraction operation is a rather costly activity from an operational point of view since great suction forces may develop at the anchor's lower interface. Hence, it is convenient that the mudmat design should be optimized to account for the service loads without imposing great difficulties on its removal (Chandler et al. [2], Chen et al. [3]).

The uplift bearing capacity of shallow foundations is a well known subject in foundation engineering theory, being object of constant revisions regarding its collapse load evaluation (e.g. Vesić [4], Rowe and Davis [5], Das and Picornell [6], Merifield et al. [7, 8], Feng et al. [9], Shen et al. [10]). In general, the collapse load of plate anchors is expressed in terms of bearing capacity factors that are obtained experimentally or numerically as a function of the parameters relevant to the problem. Inspired from Rowe and Davis [5] work, the bearing capacity factors have been mostly provided for two distinct soil/anchor interface considerations: immediate breakaway case, where the anchor's lower interface is unable to sustain tension, meaning that is no suction/adhesion at the anchor base; and no breakaway case, where the foundation material is assumed to be perfectly bonded to the base of the anchor at all stages, consequently mobilizing the foundation material beneath the anchor.

Techniques based upon limit analysis theory have proven a powerful tool for evaluating the collapse load of mechanical systems, such as foundations, beams, plates, and earth slopes, playing an important role in the design of different geostructures (Salençon [11]). In this context, the present paper aims to evaluate the uplift resistance of

shallow embedded rectangular anchors based on the theoretical framework of limit analysis and related kinematic approach.

Initially, the yield design kinematic approach is briefly presented, followed by the investigation of a class of failure mechanisms. Later, the predictions obtained are compared with available results found in literature, both for experimental and numerical data, thus validating the upper bound estimates obtained in the present work. Finally, a parametric study is conducted to assess the effect of relevant parameters upon the uplift bearing capacity of shallow anchors. .

2 Framework of analysis

2.1 Kinematic approach of limit analysis

The estimates of uplift bearing capacity of rectangular plate anchors presented in this paper are based on limit analysis techniques and its related kinematic approach, where upper bound estimates of the uplift collapse load are obtained through the analysis of failures mechanisms describing the mudmat extraction at its ultimate state. The general principle of this approach will be briefly outlined in this section.

The kinematic theorem of limit analysis presents a necessary condition for the stability of a material system under external loading. It generally states that, if there exists a kinematically admissible (KA) virtual velocity field $\hat{\underline{U}}$ (termed *failure mechanism* in the sequel) in which the virtual rate of work exerted by external forces P_{ext} exceeds the maximum resisting work P_{mr}, then the load is certainly unsafe, i.e., the system will collapse (Salençon [11], Chen [12]). Hence, for a load to be admissible, it follows that:

$$P_{ext}(\hat{\underline{U}}) \leq P_{mr}(\hat{\underline{U}}) \quad \forall \hat{\underline{U}} \text{ KA} \tag{1}$$

The term $P_{mr}(\hat{\underline{U}})$ on the right-hand side of the above inequality is the rate of maximum resisting work that is developed in the considered failure mechanism $\hat{\underline{U}}$. Its evaluation is based on the support functions Π, defined from the failure criterion of the constitutive material. The expression for $P_{mr}(\hat{\underline{U}})$ writes:

$$P_{mr}(\hat{\underline{U}}) = \int_{\Omega} \Pi\left(\hat{\underline{\underline{d}}}(\underline{x})\right) d\Omega + \int_{\Sigma} \Pi\left(\underline{n}(\underline{x}); [\hat{\underline{U}}(\underline{x})]\right) d\Sigma \tag{2}$$

where $\hat{\underline{\underline{d}}} = \frac{1}{2}\left(\nabla\hat{\underline{U}} +^t \nabla\hat{\underline{U}}\right)$ is the strain rate tensor at any point $\underline{x}$ of the material domain Ω, whereas $[\hat{\underline{U}}(\underline{x})]$ is the velocity jump when crossing a discontinuity surface Σ with normal $\underline{n}(\underline{x})$.

In the present work, the anchor is modeled as a thin rigid plate, whereas the constitutive soil material is assumed to exhibit homogeneous and isotropic strength properties according to the Tresca failure criterion with a tension cut-off. On that account, the support functions Π are evaluated for the soil mass by (Salençon [11]):

$$\Pi\left(\hat{\underline{\underline{d}}}(\underline{x})\right) = C\left(|\hat{d}_1| + |\hat{d}_2| + |\hat{d}_3| - \operatorname{tr}\hat{\underline{\underline{d}}}\right) + T \operatorname{tr}\hat{\underline{\underline{d}}} \qquad \text{if} \quad \operatorname{tr}\hat{\underline{\underline{d}}} \geq 0 \tag{3a}$$

$$\Pi\left(\underline{n}(\underline{x}); [\hat{\underline{U}}(\underline{x})]\right) = C\left(|[\hat{\underline{U}}]| - [\hat{\underline{U}}] \cdot \underline{n}\right) + T[\hat{\underline{U}}] \cdot \underline{n} \qquad \text{if} \quad [\hat{\underline{U}}] \cdot \underline{n} \geq 0 \tag{3b}$$

where C is the material cohesion, T is the tension stress limit, and $\hat{d}_1$, $\hat{d}_2$ and $\hat{d}_3$ are the eigenvalues of the strain rate tensor $\hat{\underline{\underline{d}}}$. The requirements stated on Eqs. 3a and 3b are the pertinence conditions of the failure criteria, which allows to construct relevant velocity fields for the failure mechanisms with finite values of Π.

The interface between the anchor's bottom and foundation soil mass is considered purely cohesive, being determined by a tensile stress threshold t_i in order to simulate any adhesion effects that may develop during the extraction process. Hence, the support function for the interface strength is written as:

$$\Pi\left(\underline{n}; [\hat{\underline{U}}]\right) = t_i[\hat{\underline{U}}] \cdot \underline{n} \qquad \text{if} \quad [\hat{\underline{U}}] \cdot \underline{t} = 0 \quad \text{and} \quad [\hat{\underline{U}}] \cdot \underline{n} \geq 0 \tag{4}$$

where $\underline{t}$ is the unit tangent vector to the surface.

2.2 Failure mechanism

The class of failure mechanisms under analysis consists of a rectangular plate anchor with base $2B$ and length $2L$ installed at a depth H being continuously pullout from the soil mass with a constant velocity $[\hat{\underline{U}}] = U\underline{e}_z$ under a pullout force $\underline{F} = F\underline{e}_z$ applied on the anchor's centroid until its collapse. Initially, the interface soil/anchor is considered perfectly adherent ($t_i = \infty$), so that portions of the soil both above and beneath the anchor will move

along with the anchor in a rigid body motion. Consequently, discontinuity velocity surfaces will be developed in the soil mass, which can be described in cylindrical coordinates by the generic functions $z = f_{sup}(r, \theta)$ and $z = g_{sup}(r, \theta)$ for the discontinuities above the anchor, and by $z = f_{inf}(r, \theta)$ and $z = g_{inf}(r, \theta)$ for the discontinuities beneath the anchor. Figure 1 presents a schematic view of such discontinuities surfaces for only a quarter of the rectangular plate given the model symmetry.

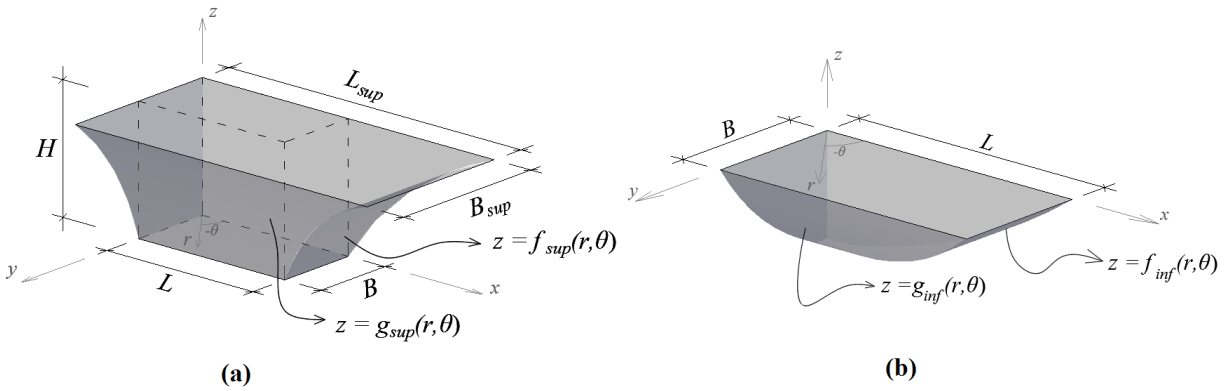

Figure 1. Discontinuity surfaces (a) above and (b) beneath the anchor.

In the proposed failure mechanism, the rate of work performed by the external forces is developed by the pullout force F and the weight of material mobilized in the failure mechanism, while P_{mr} is characterized only by Eq. 3b, since the proposed mechanism does not involve any strain rate components. The upper bound pullout force can then be written as a sum of two components such that:

$$F \leq F_{sup} + F_{inf} \tag{5}$$

where F_{sup} is due to the contribution from the discontinuities above the anchor and F_{inf} from beneath the anchor. Applying the kinematic theorem expressed by Eq. 1, such components of the pullout force can then be written for the proposed failure mechanism as:

$$\begin{aligned}\frac{F_{sup}}{4} = \gamma BLH + \int_0^{\phi}\int_{L/\cos\theta}^{L_{sup}/\cos\theta}\left[C\sqrt{1+f_{sup,r}^2+\frac{f_{sup,\theta}^2}{r^2}} + T - C + \gamma(H - f_{sup})\right] r dr d\theta \quad + \\ \int_0^{\frac{\pi}{2}-\phi}\int_{B/\cos\theta}^{B_{sup}/\cos\theta}\left[C\sqrt{1+g_{sup,r}^2+\frac{g_{sup,\theta}^2}{r^2}} + T - C + \gamma(H - g_{sup})\right] r dr d\theta\end{aligned} \tag{6a}$$

$$\begin{aligned}\frac{F_{inf}}{4} = \int_0^{\phi}\int_0^{L/\cos\theta}\left[C\sqrt{1+f_{inf,r}^2+\frac{f_{inf,\theta}^2}{r^2}} + T - C - \gamma f_{inf}\right] r dr d\theta \quad + \\ \int_0^{\frac{\pi}{2}-\phi}\int_0^{B\cos\theta}\left[C\sqrt{1+g_{inf,r}^2+\frac{g_{inf,\theta}^2}{r^2}} + T - C - \gamma g_{inf}\right] r dr d\theta\end{aligned} \tag{6b}$$

where $\phi = \arctan(B/L)$, γ is the soil unit weight, $f_{sup,x} = \frac{\partial f_{sup}}{\partial x}$ with $x = r, \theta$ (same definitions are used for g_{sup} and g_{inf}). The function dependence on the independent variable was omitted by simplicity. Equations 6a and 6b describe a functional form upper bound solution for F computed from the geometry of discontinuity surfaces. Hence, the minimization of F with respect to those functions will lead to an optimal estimate of this quantity. Applying the Euler-Lagrange equation to Eq. 6a, the following nonlinear second-order differential equations are obtained:

$$\begin{aligned}&\frac{f_{sup,r}\left(r^2 f_{sup,r} f_{sup,rr} + f_{sup,\theta} f_{sup,r\theta} - \frac{f_{sup,\theta}^2}{r}\right) + f_{sup,\theta}\left(f_{sup,r} f_{sup,\theta} + \frac{f_{sup,\theta} f_{sup,\theta\theta}}{r^2}\right)}{r\left(1 + f_{sup,r}^2 + \frac{f_{sup,\theta}^2}{r^2}\right)^{3/2}} - \\ &\frac{r\left(r f_{sup,rr} + f_{sup,r}\right) + f_{sup,\theta\theta}}{r\sqrt{1 + f_{sup,r}^2 + \frac{f_{sup,\theta}^2}{r^2}}} + \frac{\gamma r}{C} = 0\end{aligned} \tag{7a}$$

$$\frac{g_{sup,r}\left(r^2 g_{sup,r} g_{sup,rr} + g_{sup,\theta} g_{sup,r\theta} - \frac{g_{sup,\theta}^2}{r}\right) + g_{sup,\theta}\left(g_{sup,r} g_{sup,\theta} + \frac{g_{sup,\theta} g_{sup,\theta\theta}}{r^2}\right)}{r\left(1 + g_{sup,r}^2 + \frac{g_{sup,\theta}^2}{r^2}\right)^{3/2}} - \frac{r\left(r g_{sup,rr} + g_{sup,r}\right) + g_{sup,\theta\theta}}{r\sqrt{1 + g_{sup,r}^2 + \frac{g_{sup,\theta}^2}{r^2}}} + \frac{\gamma r}{C} = 0 \tag{7b}$$

while the differential equations with respect to the discontinuities beneath the anchor can be obtained simply by substituting f_{sup} and g_{sup} by f_{inf} and g_{inf}, respectively, in the above equations. The solution for the discontinuity surfaces must comply with following boundary conditions:

$$f_{sup}(L/\cos\theta, \theta) = f_{inf}(L/\cos\theta, \theta) = 0 \quad \forall\theta \in [0, \phi] \tag{8a}$$

$$g_{sup}(B/\cos(\theta), \theta) = g_{inf}(B/\cos(\theta), \theta) = 0 \quad \forall\theta \in [0, \pi/2 - \phi] \tag{8b}$$

$$f_{sup}(L_{sup}/\cos\theta, \theta) = H \quad \forall\theta \in [0, \phi] \tag{8c}$$

$$g_{sup}(B_{sup}/\cos\theta, \theta) = H \quad \forall\theta \in [0, \pi/2 - \phi] \tag{8d}$$

$$f_{sup,r}(r, 0) = 0 \quad \forall r \in [L, L_{sup}]; \quad g_{sup,r}(r, \pi/2) = 0 \quad \forall r \in [B, B_{sup}] \tag{8e}$$

$$f_{inf,r}(r, 0) = 0 \quad \forall r \in [0, L]; \quad g_{inf,r}(r, \pi/2) = 0 \quad \forall r \in [0, B] \tag{8f}$$

$$f_{sup}(r, \phi) = g_{sup}(r, \pi/2 - \phi) \quad \text{and} \quad f_{inf}(r, \phi) = g_{inf}(r, \pi/2 - \phi) \quad \forall r \tag{8g}$$

$$B_{sup} = L_{sup} \tan\phi \tag{8h}$$

The value for L_{sup} (Fig. 1) is initially unknown, so it will be assumed as a minimization parameter given that all solutions lead to an upper bound estimate of the collapse load. Figure 2 presents an example of a solution obtained for the discontinuity surfaces proposed.

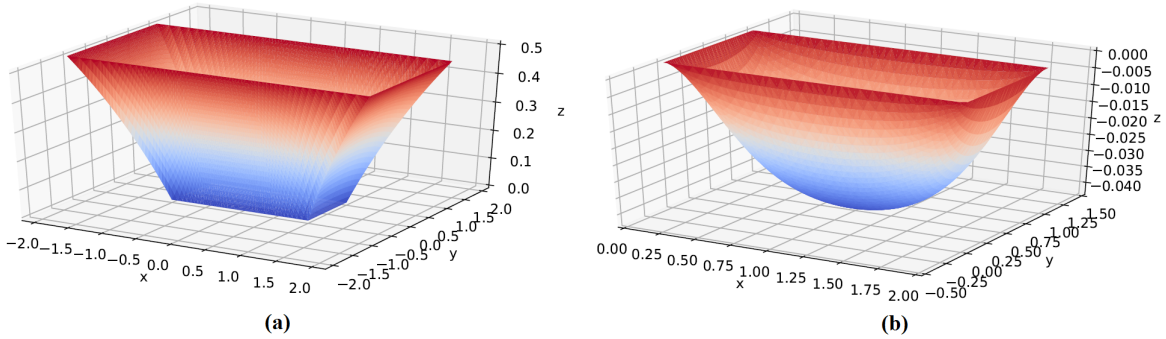

Figure 2. Example of discontinuity surfaces obtained in the proposed class of failure mechanisms: (a) above and (b) beneath the anchor.

Taking into account the possibility of an interface with a tensile stress threshold such as described by Eq. 4, the upper bound pullout force for the proposed mechanism can be written as:

$$F \leq F_{sup} + \min\left(F_{inf}, 4BLT, 4BLt_i\right) \tag{9}$$

The second term on the right-hand side of Eq. 9 states that the anchor breakout may occur by mobilizing either the tensile strength of the foundation material or the interface strength (vanishing volume shown in Fig. 2(b))

3 Model results

This section aims to present results for the upper bound collapse load obtained by the proposed class of failure mechanisms through the limit analysis kinematic approach. The governing differential equations presented in subsection 2.2 were solved numerically by a finite difference scheme, adopting the Newton-Raphson method to cope with the nonlinear systems. The minimization with respect to L_{sup} was also conducted numerically through a grid of points to find the function's global minimum.

3.1 Comparison with available results

Employing the limit analysis static approach, Merifield et al. [8] presented lower bound estimates for the collapse load of rectangular plate anchors. The results were obtained numerically through a finite difference discretization of the problem, where the soil was modeled as a homogeneous and isotropic conventional Tresca material ($T = \infty$), whereas the interface was considered unable to sustain tension: $t_i = 0$ (*immediate breakaway case*). Results obtained by the authors are compared with the present work in Fig. 3 for rectangular anchors with aspect ratios $L/B = 1$, 2, and 4. It can be seen that, for embedment ratio $H/B = 1$, the present upper bound estimates are very close to the lower bound estimate derived by Merifield et al. [8], while the difference between approaches increases as the embedment depth increases. Even though the results from Merifield et al. [8] constitute a lower bound estimate while the present study is an upper bound estimate, this difference is mainly attributed due to the fact that the proposed collapse mechanism is not representative of deeper anchors pullout failure, thus supporting its application for shallowly embedded mudmats.

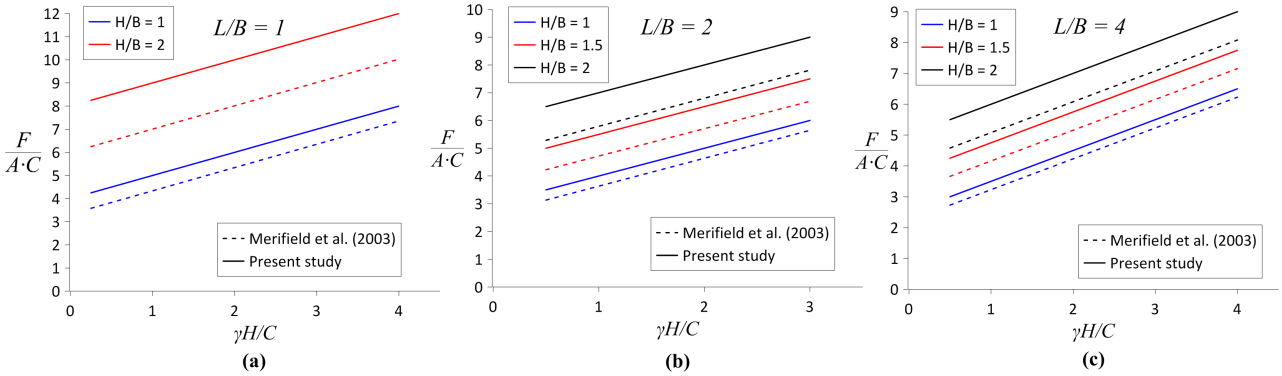

Figure 3. Comparison of the present study results with finite-element data from Merifield et al. [8] for rectangular anchors with aspect ratios: (a) L/B = 1, (b) L/B = 2 and (c) L/B = 4.

Singh and Ramaswamy [13] present a series of experimental data from pullout tests conducted on laboratory with a clayey soil varying the anchor's aspect ratio and embedment depth. Figure 4 displays a comparison between the experimental data from Singh and Ramaswamy [13] and the present study, where the region of results was plotted varying T from 0 to C given the lack of information about the clay adopted in the tests. It is seen that the upper bound predictions are in good agreement for low embedment ratios, usually smaller than 2, thus validating its application for very shallow anchors as proposed.

3.2 Parametric analysis

Considering the case where the interface resistance is null ($t_i = 0$), the breakout occurs without mobilizing any resistance of the foundation mass, and therefore $F_{inf} = 0$. In this case, Figure 5 presents the variations of the pullout bearing capacity F/AC as a function of $\gamma H/C$ for three difference embedment ratios ($H/B = 0.5$, 1 and 2), three aspect ratios ($L/B = 1$, 2 and 5), and considering the cases where $T = 0$ and $T \geq C$. It can be seen that in general, the anchor bearing capacity increases with $\gamma H/C$, presenting a slightly nonlinear increase for $\gamma H/C \leq 1$ for $T = 0$, while for the case where $T \geq C$, a linear increase is observed. For the latter case, the discontinuity surfaces above the anchor reduce to vertical planes, hence the upper bound collapse load is independent of T, and can be expressed as:

$$F \leq 4\,(L + B)\,HC + 4\gamma BLH \tag{10}$$

Considering an interface with $t_i = C$, the breakout occurs depending on the parameters magnitude. For instance, when $T = 0$, the results obtained will be the same as displayed in Fig. 5 since the collapse takes place without mobilizing the interface resistance. For the case when $t_i = T = C$, Fig. 6 presents the upper bound estimated obtained through the optimized failure mechanism proposed, obtained by solving the governing differential equation. A comparison with the results obtained considering the interface resistance (neglecting F_{inf} from Eq. 6b) is also presented. Since the superior discontinuity surface is always described by vertical planes in those cases, the difference observed is only due to how the discontinuity surface beneath the anchor develops. It can be seen that the optimal mechanism presented lower estimates for the upper bound extraction load of rectangular

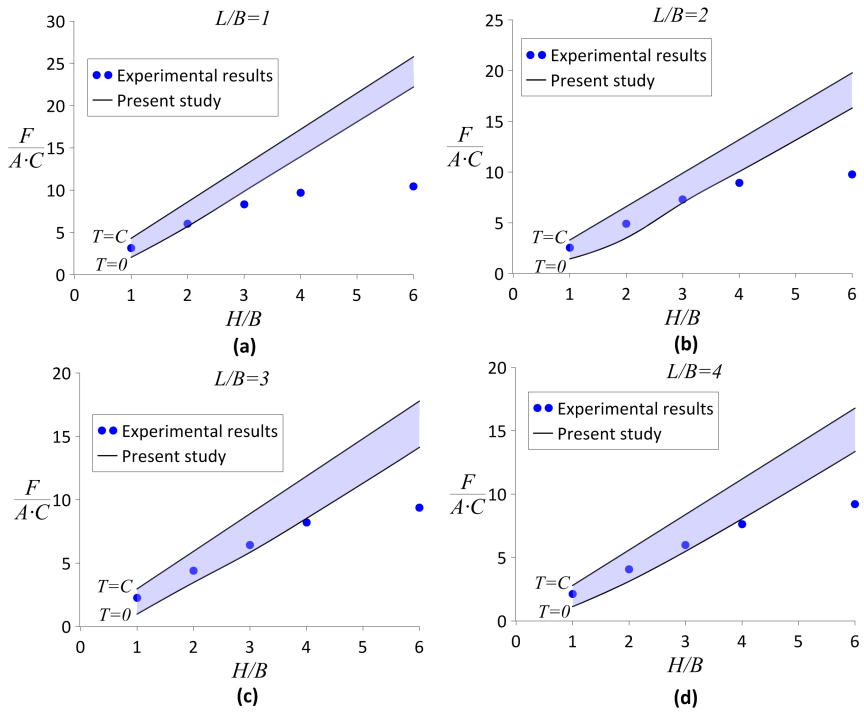

Figure 4. Comparison of the present study results with experimental data from Singh and Ramaswamy [13] for rectangular anchors with aspect ratios: (a) L/B = 1, (b) L/B = 2 and (c) L/B = 4.

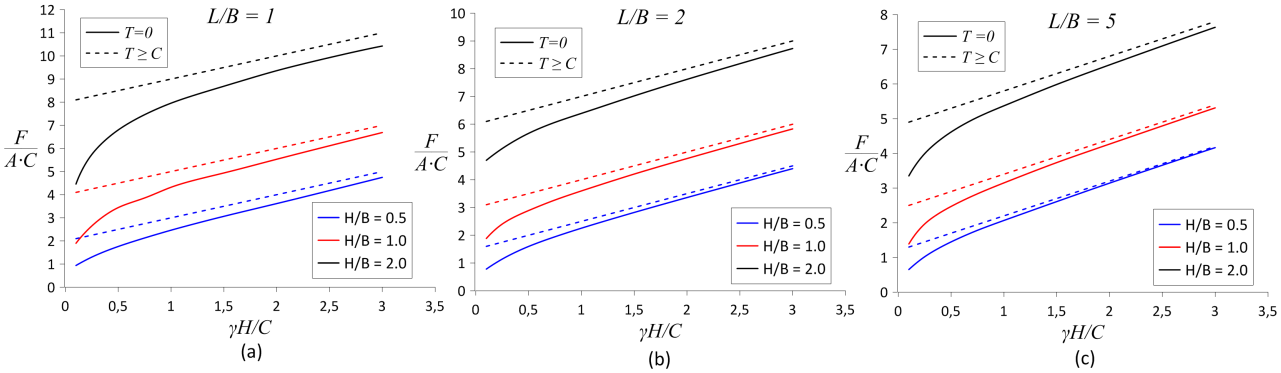

Figure 5. Parametrical study for rectangular anchors with no interface resistance ($t_i = 0$) and aspect ratios: (a) L/B = 1, (b) L/B = 2 and (c) L/B = 5.

anchors, with the difference being more pronounced with an increase in $\gamma H/C$ and L/B.

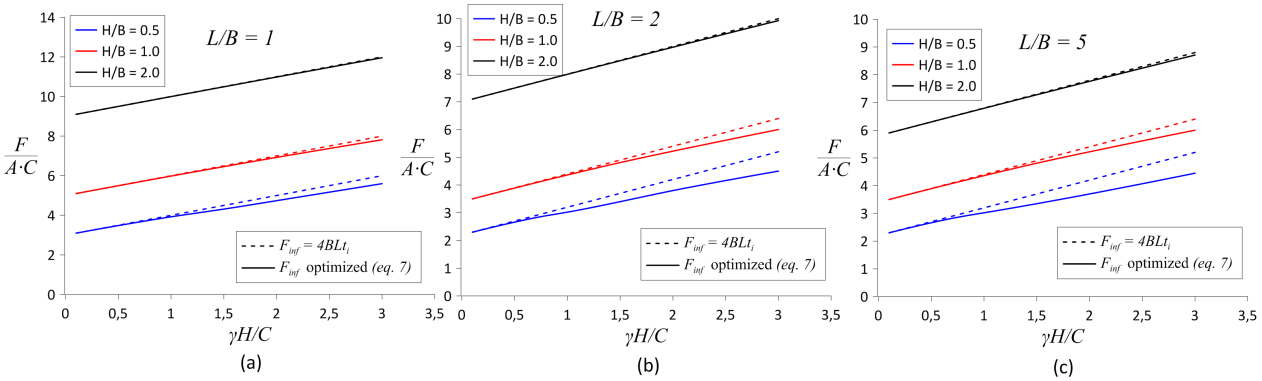

Figure 6. Parametrical study for rectangular anchors with $t_i = T = C$ and aspect ratios: (a) L/B = 1, (b) L/B = 2 and (c) L/B = 5.

For the cases such as the ones presented in Fig. 6, the upper bound collapse load can be estimated as:

$$F \leq 4HC\,(B+L) + 4\gamma BL + \min\left(4BLt_i, 4BLT, F_{inf}\right) \tag{11}$$

4 Conclusions

The present paper describes an application of the limit analysis kinematic approach to obtain estimates of the pullout bearing capacity of very shallow rectangular anchors embedded in a cohesive soil, thus providing upper bound reference values for the breakout load with account for the material's tension limit and interface resistance. A class of failure mechanisms is explored and the best upper bound estimate is obtained from optimization of a non-convex functional involving the parameters defining the geometry of discontinuities surfaces. In that respect, the solutions to governing minimization differential equations are obtained numerically.

The model predictions were compared with available numerical and experimental results found in the literature. It is concluded that for small values of embedment ratio, such as the ones encountered in the offshore foundation practice, the solution of the present study shows itself a good tool to estimate the pullout capacity load, as for deeper anchors a more suitable mechanism should be investigated.

A parametric analysis was conducted varying the main parameters of the mechanical problem. It is shown that the pullout bearing capacity is mainly affected by the material resistance, embedment ratio, and interface conditions, highlighting that the material tension resistance plays a key role in the anchor capacity.

Acknowledgements. The authors gratefully appreciate the support provided by the Coordination for the Improvement of Higher Education Personnel (CAPES) and the Federal University of Rio Grande do Sul.

Authorship statement. The authors hereby confirm that they are the sole liable persons responsible for the authorship of this work, and that all material that has been herein included as part of the present paper is either the property (and authorship) of the authors, or has the permission of the owners to be included here.

References

[1] M. F. Randolph, C. Gaudin, S. M. Gourvenec, D. J. White, N. Boylan, and M. J. Cassidy. Recent advances in offshore geotechnics for deep water oil and gas developments. *Ocean Engineering*, vol. 38, n. 7, pp. 818–834, 2011.

[2] J. Chandler, D. White, E. J. Techera, S. Gourvenec, and S. Draper. Engineering and legal considerations for decommissioning of offshore oil and gas infrastructure in Australia. *Ocean Engineering*, vol. 131, pp. 338–347, 2017.

[3] R. Chen, C. Gaudin, and M. Cassidy. Investigation of the vertical uplift capacity of deep water mudmats in clay. *Canadian Geotechnical Journal*, vol. 49, n. 7, pp. 853–865, 2012.

[4] A. S. Vesić. Breakout Resistance of Objects Embedded in Ocean Bottom. *Journal of Soil Mechanical Foundation*, vol. 97, n. 9, pp. 1183–1205, 1971.

[5] R. K. Rowe and E. H. Davis. The behaviour of anchor plates in clay. *Géotechnique*, vol. 32, n. 1, pp. 9–23, 1982.

[6] B. M. Das and M. Picornell. Ultimate Resistance of Vertical Plate Anchors in Clay. In *Coastal Engineering 1986*, pp. 1831–1842, Taipei, Taiwan. American Society of Civil Engineers, 1987.

[7] R. S. Merifield, S. W. Sloan, and H. S. Yu. Stability of plate anchors in undrained clay. *Géotechnique*, vol. 51, n. 2, pp. 141–153, 2001.

[8] R. S. Merifield, A. V. Lyamin, S. W. Sloan, and H. S. Yu. Three-Dimensional Lower Bound Solutions for Stability of Plate Anchors in Clay. *Journal of Geotechnical and Geoenvironmental Engineering*, vol. 129, n. 3, pp. 243–253, 2003.

[9] X. Feng, M. Randolph, S. Gourvenec, and R. Wallerand. Design approach for rectangular mudmats under fully three-dimensional loading. *Géotechnique*, vol. 64, n. 1, pp. 51–63, 2014.

[10] Z. Shen, X. Feng, and S. Gourvenec. Effect of interface condition on the undrained capacity of subsea mudmats under six-degree-of-freedom loading. *Géotechnique*, vol. 67, n. 4, pp. 338–349, 2017.

[11] J. Salençon. *Calcul à la rupture et analyse limite*. Presses de l'école nationale des Ponts et chaussées, Paris, 1983.

[12] W.-F. Chen. *Limit analysis and soil plasticity*, volume 1. Elsevier, Amsterdan, 1 edition, 1975.

[13] S. P. Singh and S. V. Ramaswamy. Effect of shape on holding capacity of plate anchors buried in soft soil. *Geomechanics and Geoengineering*, vol. 3, n. 2, pp. 145–154, 2008.